

# Blind Selected Mapping using 2-level Phase Rotation Set and 2-step Phase Rotation Sequence Estimation based on the Fourth-power Constellation

Amnart Boonkajay<sup>†</sup> and Fumiyuki Adachi<sup>‡</sup>

<sup>† ‡</sup> Research Organization of Electrical Communication (ROEC), Tohoku University

2-1-1 Katahira, Aoba-ku, Sendai, Miyagi, 980-8577 Japan

E-mail: <sup>†</sup>amnart@riec.tohoku.ac.jp <sup>‡</sup>adachi@ecei.tohoku.ac.jp

**Abstract** Blind selected mapping (blind SLM) is an effective peak-to-average power ratio (PAPR) reduction technique which does not require side information sharing. In the blind SLM, the receiver employs phase rotation sequence estimation, which can be carried out using maximum-likelihood (ML) estimation or 2-step sequence estimation using Viterbi algorithm. Recently, we showed that the use of codebook generated from a 2-level phase rotation set  $\{0^\circ, 135^\circ\}$  and the ML phase rotation sequence estimation based on the fourth-power QAM constellation requires much less complexity compared to the conventional blind SLM. However, when the number of phase rotation sequences is large, the computational complexity remains high. In this paper, we introduce a 2-level phase rotation set  $\{0^\circ, 135^\circ\}$  and the 2-step sequence estimation using Viterbi algorithm to a blind SLM. It is found that the use of 2-level phase rotation set significantly reduce the number of branches and states in the Viterbi algorithm and hence, leads to complexity reduction. Simulation results confirm that the blind SLM using the 2-level phase rotation set and the 2-step sequence estimation effectively lowers the PAPR and achieves similar BER to the ML sequence estimation with less computational complexity.

**Keyword** Peak-to-average power ratio (PAPR), OFDM, single carrier (SC), selected mapping (SLM)

## 1. Introduction

The design of low peak-to-average power ratio (PAPR) waveforms remains important even in the fifth-generation (5G) mobile communication to achieve high energy efficiency, especially for user equipments (UEs) [1]. Single carrier (SC) signals typically have lower PAPR than orthogonal frequency division multiplexing (OFDM) signals [2]. However, PAPR of SC signals increases due to transmit processing such as band-limit filtering, precoding and high-level data modulation [3], indicating that PAPR reduction is also necessary for SC transmission.

We have been studying a PAPR reduction technique called blind selected mapping (blind SLM) [4]. Blind SLM can lower the PAPR effectively by multiplying the original data symbol sequence with a phase rotation sequence. The phase rotation sequence is selected from a codebook consisting of random sequences generated from a set  $\{0^\circ, 120^\circ, 240^\circ\}$  [4]. The receiver needs to estimate the phase rotation sequence which has been used at the transmitter side in order to carry out data de-modulation. The blind SLM in [4] is compatible with both OFDM and SC signals. Its applications to multiple-input multiple-output (MIMO) transmissions, such as space-time block coded transmit diversity (STBC-TD) and multiuser MIMO (MU-MIMO), were introduced in [5] and [6], respectively.

The phase rotation sequence estimation in [4-6] is the maximum likelihood (ML) estimation based on minimum Euclidean distance between the de-mapped symbols and the original signal constellation. It works effectively, however, requires high computational complexity. A 2-step phase rotation sequence estimation using Viterbi

algorithm [7] was proposed to reduce the complexity, but its capability is obvious only when the number of phase rotation sequences is high. Recently, we showed that the use of codebook generated from a 2-level phase rotation set  $\{0^\circ, 135^\circ\}$  and the ML phase rotation sequence estimation based on the fourth-power QAM constellation [8,9] requires less computational complexity than those of [4-7]. This is because the number of signal points in the fourth-power constellation is much less than the original QAM, leading to reduced number of candidates in minimum Euclidean distance search. It is shown in [9] that the new ML phase rotation sequence estimation achieves less computational complexity while keeping the same bit error rate (BER) as the conventional blind SLM in [4-6]. However, since the complexity of the ML estimation in [9] monotonically increases as the number of phase rotation sequences increases, the complexity becomes higher than the 2-step estimation in [7].

Meanwhile, the 2-step sequence estimation using Viterbi algorithm in [7] was designed and evaluated using 3-level phase rotation set. The results of [7] encourage us to use Viterbi algorithm in the sequence estimation. Hence, in this paper, to further reduce the computational complexity, we apply 2-level phase set  $\{0^\circ, 135^\circ\}$  to the blind SLM with 2-step sequence estimation using Viterbi algorithm and the fourth-power QAM constellation. The use of fourth-order constellation reduces the number of possible paths to be considered during survival path searching. Furthermore, the use of 2-level phase set significantly reduces the number of branches and states in the Viterbi algorithm compared to [7]. These reasons lead

to complexity reduction. In this paper, the new blind SLM is called a *modified blind SLM* in short.

Performance evaluation of the modified blind SLM is carried out in terms of PAPR, BER and computational complexity by computer simulation assuming single-user SC uplink transmission using single-antenna transmission (SISO) and STBC-TD. The simulation results confirm that the blind SLM using the 2-level phase rotation set and the 2-step sequence estimation effectively lowers the PAPR and achieves low-complexity receiver even when the number of phase rotation sequences is high, while keeping the BER similar to the ML estimation.

The rest of this paper is organized as follows. Section 2 provides an overview of blind SLM. Sect. 3 introduces the 2-step sequence estimation using the fourth-power constellation. Sect. 4 shows computer simulation results and discussion. Finally, Sect. 5 concludes the paper.

## 2. Overview of the blind SLM

Here, we briefly describe the concept of blind SLM in [4-7]. For simplicity, we describe only the signal representation for STBC-TD, where the representation for SISO is obtained by setting the number of base station (BS) antennas ( $N_{BS}$ ) and UE antennas ( $N_{UE}$ ), STBC coding parameters  $J$  and  $Q$ , and STBC coding rate  $R_{STBC}=J/Q$ , to be 1. The number of transmit antennas ( $N_t$ ) becomes  $N_{BS}$  for OFDM downlink and  $N_{UE}$  for SC uplink, respectively. We describe the system model for both OFDM downlink and SC uplink, however, only the performance of SC uplink is available in Sect. 4. We assume that STBC-TD with transmit filtering is used in the OFDM downlink, while the STBC-TD without transmit filtering is used in SC uplink. The transceiver models with blind SLM can be depicted by Fig. 1.

### 2.1. SLM algorithm

Assuming that a time-domain transmit waveform is  $\{s(n); n=0 \sim N_c-1\}$ , PAPR is calculated over a  $V$ -times oversampled block and is given by

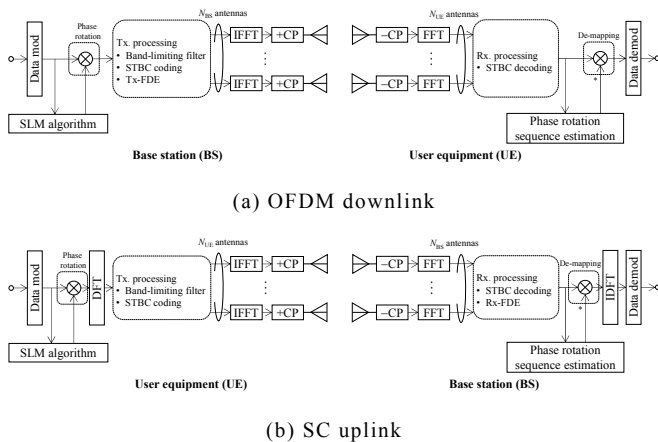


Fig. 1 Transceiver models equipped with blind SLM.

$$\text{PAPR}(\{s(n)\}) = \frac{\max\{|s(n)|^2, n=0, \frac{1}{V}, \frac{2}{V}, \dots, N_c-1\}}{\frac{1}{N_c} \sum_{n=0}^{N_c-1} |s(n)|^2}. \quad (1)$$

In STBC-TD transmission, the  $j$ -th block of an  $N_c$ -length data block  $\{d_j(n); n=0 \sim N_c-1, j=0 \sim J-1\}$  is phase-rotated by multiplying with the phase rotation sequence  $\{\Phi_{\hat{m}}(n); n=0 \sim N_c-1\}$ , yielding the phase rotated block  $\{d_{j,\hat{m}}(n); n=0 \sim N_c-1, j=0 \sim J-1\}$ . In the SC uplink,  $\{d_{j,\hat{m}}(n)\}$  is transformed to frequency components block  $\{D_{j,\hat{m}}(k); k=0 \sim N_c-1\}$  by  $N_c$ -point discrete Fourier transform (DFT). In the OFDM downlink, we simply obtain  $\{D_{j,\hat{m}}(k)\} = \{d_{j,\hat{m}}(k)\}$ . Then  $\{D_{j,\hat{m}}(k)\}$  are passed through transmit signal processing e.g. STBC coding and/or transmit filtering, obtaining the frequency-domain transmit signal at the  $n_i$ -th transmit antenna ( $n_i=0 \sim N_t-1$ ) and the  $q$ -th timeslot as  $\{S_{n_i,q,\hat{m}}(k); k=0 \sim N_c-1\}$  and its corresponding time-domain waveform after applying inverse DFT (IDFT) as  $\{s_{n_i,q,\hat{m}}(n); n=0 \sim N_c-1\}$ . If we assume that  $N_{UE}=2$ ,  $S_{n_i,q,\hat{m}}(k)$  can be described by the following matrix representations.

$$\begin{bmatrix} S_{0,0,\hat{m}}(k) & S_{0,1,\hat{m}}(k) \\ S_{1,0,\hat{m}}(k) & S_{1,1,\hat{m}}(k) \end{bmatrix} = \sqrt{\frac{2E_s}{T_s}} \begin{bmatrix} D_{0,\hat{m}}(k) & -D_{1,\hat{m}}^*(k) \\ D_{1,\hat{m}}(k) & D_{0,\hat{m}}^*(k) \end{bmatrix} \quad \text{for SC uplink,} \quad (2a)$$

$$\begin{bmatrix} S_{0,0,\hat{m}}(k) & S_{0,1,\hat{m}}(k) \\ \vdots & \vdots \\ S_{N_{BS}-1,0,\hat{m}}(k) & S_{N_{BS}-1,1,\hat{m}}(k) \end{bmatrix} = \sqrt{\frac{2E_s}{T_s}} \mathbf{W}_T(k) \begin{bmatrix} D_{0,\hat{m}}(k) & -D_{1,\hat{m}}^*(k) \\ D_{1,\hat{m}}(k) & D_{0,\hat{m}}^*(k) \end{bmatrix} \quad \text{for OFDM downlink,} \quad (2b)$$

where  $\mathbf{W}_T(k)$  is the transmit filtering [5].  $E_s$  and  $T_s$  are symbol energy and symbol duration, respectively.

In the case of SC uplink STBC-TD, the PAPR of signals before and after STBC coding are exactly the same. This is because the STBC coding employs only complex conjugate operations [5]. Therefore, we can select an individual phase rotation sequence for each of  $\{d_j(n)\}$ . The selected sequence for the  $j$ -th data block,  $\{\Phi_{\hat{m}(j)}(n)\}$  with the sequence index  $\hat{m}(j)$ , is determined by

$$\hat{m}(j) = \arg \min_{m=0 \sim M-1} (\text{PAPR}(\{\Phi_m(n)d_j(n)\})), \quad (3)$$

where  $\{\Phi_m(n); n=0 \sim N_c-1, m=0 \sim M-1\}$  is the  $m$ -th phase rotation sequence in a predefined codebook and is generated randomly as  $\Phi_m(n) \in \{e^{i0}, e^{i(3\pi/4)}\}$  (equivalent to  $\{0^\circ, 135^\circ\}$ ), except the first sequence is defined as  $\{\Phi_0(n)=1; n=0 \sim N_c-1\}$  to represent the original signal.

Meanwhile, Eq. (3) is not available for STBC-TD with transmit filtering since the signals before and after transmit filtering have different PAPR. In this case, a selection criterion which minimizes the maximum PAPR value (called Mini-max criterion) among all  $N_t$  transmit antennas is used as follows.

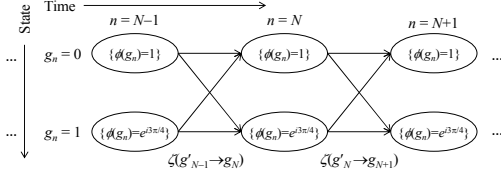
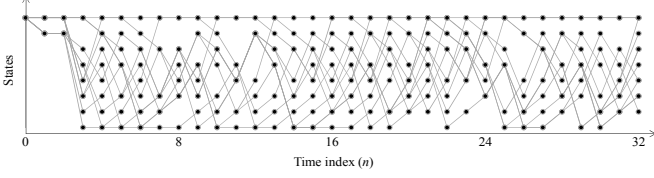
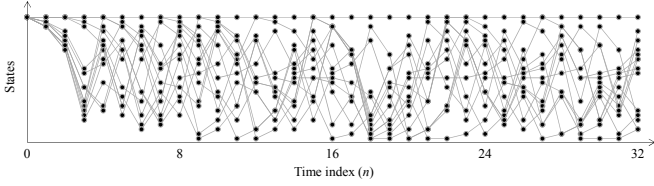


Fig. 2 Illustration of 2-state trellis.



(a) 2-level phase set with  $G_{\max}=8$



(b) 3-level phase set with  $G_{\max}=27$

Fig. 3 An example of trellis diagram with reduced branches ( $N_c=32$  and  $M=16$ ).

$$\hat{m} = \arg \min_{m=0 \sim M-1} \left( \max_{\substack{n_r=0 \sim N_r-1 \\ q=0 \sim Q-1}} \text{PAPR}(\{s_{n_r, q, m}(n)\}) \right), \quad (4)$$

The selection criterion in Eq. (4) is sub-optimal and hence, PAPR increases when  $N_t$  increases. However, it can keep the phase rotation estimation simple and no major changes on filtering weights calculation is required. Note that the criterion in Eq. (4) is also used for MU-MIMO [6].

## 2.2. Phase rotation sequence estimation

Phase rotation sequence estimation is employed after the receive signal processing by calculating Euclidean distance between the de-mapped signal (i.e. multiplied by  $\{\Phi_{m(j)}^*(n); n=0 \sim N_c-1\}$ ) and original constellation. If the de-mapping is done correctly, the de-mapped signal should be very close to the original constellation and hence, its distance from the nearest QAM symbol is very small. The phase rotation sequence associated with the de-mapped signal having the minimum averaged distance is selected.

In STBC-TD, assuming the  $j$ -th time-domain received block after employing receive processing (i.e., MMSE-FDE, STBC decoding and IDFT for SC uplink, and only STBC decoding for OFDM downlink) and before de-mapping is  $\{\hat{d}_j(n); n=0 \sim N_c-1, j=0 \sim J-1\}$ , the phase rotation sequence estimation can be expressed as

$$\tilde{m}(j) = \arg \min_{m=0 \sim M-1} \left( \sum_{n=0}^{N_c-1} \min_{c \in \Psi_{\text{mod}}} \|\Phi_m^*(n) \hat{d}_j(n) - c\| \right), \quad (5)$$

where  $\Psi_{\text{mod}}$  represents the original data modulated constellation (i.e. QAM mapping) and  $\|\cdot\|$  represents Euclidean norm. Eq. (5) can be carried out based on either

ML [4] or Viterbi algorithm [7]. Meanwhile, when the phase rotation set  $\{0^\circ, 135^\circ\}$  is used, we can relax Eq. (5) by considering the distance between the fourth-order of the de-mapped symbols and the fourth-order of QAM symbols [8,9], which is

$$\tilde{m}(j) = \arg \min_{m=0 \sim M-1} \left( \sum_{n=0}^{N_c-1} \min_{c \in \Psi_{\text{mod}}^4} \left| \text{Re} \left\{ \left( \Phi_m^*(n) \hat{d}_j(n) \right)^4 \right\} - \text{Re} \{c\} \right| \right), \quad (6)$$

where  $\Psi_{\text{mod}}^4$  is a set of fourth-power QAM constellation. The size of  $\Psi_{\text{mod}}^4$  is generally much less than that of  $\Psi_{\text{mod}}$  because of an existence of complex-conjugated pairs in  $\Psi_{\text{mod}}$ . The above fact contributes to complexity reduction. Although (6) achieves low-complexity phase rotation sequence estimation, it still needs to compute the norm for all phase rotation sequences, resulting in high complexity when  $M$  is large.

## 3. 2-step estimation using the fourth-power constellation

A modification of 2-step sequence estimation by considering the fourth-order constellation is expected to keep complexity of blind SLM receiver low in every  $M$ . Here, we describe the modified 2-step sequence estimation by dividing this session to 2 parts; Viterbi algorithm and sequence verification. Since the phase rotation sequence estimation is done for one received block, we ignore the index  $j$  in STBC-TD for simplicity. Here below, the Viterbi algorithm is used to estimate the phase rotation only, where the data decision is not included.

### 3.1. Viterbi algorithm

Firstly, we define an objective function with objective metric  $\varepsilon$  based on (6). By ignoring the codebook and assuming that  $\Phi_{\text{SLM}}$  is a set of possible phase rotation  $\{e^{j0}, e^{i(3\pi/4)}\}$ ,  $\varepsilon$  is expressed by

$$\varepsilon = \sum_{n=0}^{N_c-1} \min_{\substack{\phi(n) \in \Phi_{\text{SLM}} \\ c \in \Psi_{\text{mod}}^4}} \left| \text{Re} \left\{ \left( \phi^*(n) \hat{d}(n) \right)^4 \right\} - \text{Re} \{c\} \right|. \quad (7)$$

Then,  $\varepsilon$  at time index  $n=N$ ,  $0 \leq N \leq N_c-1$  is expressed by

$$\begin{aligned} \varepsilon(N) &= \sum_{n=0}^{N-1} \min_{\substack{\phi(n) \in \Phi_{\text{SLM}} \\ c \in \Psi_{\text{mod}}^4}} \left| \text{Re} \left\{ \left( \phi^*(n) \hat{d}(n) \right)^4 \right\} - \text{Re} \{c\} \right| \\ &= \varepsilon(N-1) + \min_{\substack{\phi(N) \in \Phi_{\text{SLM}} \\ c \in \Psi_{\text{mod}}^4}} \left| \text{Re} \left\{ \left( \phi^*(N) \hat{d}(N) \right)^4 \right\} - \text{Re} \{c\} \right| \end{aligned} \quad (8)$$

By using Eq. (8), we can search an optimal phase rotation sequence  $\{\Phi_{\text{opt}}(n); n=0 \sim N_c-1\}$  by using Viterbi algorithm [7,10]. We assume that  $g_n$  represents the  $g$ -th state ( $g=0 \sim G_{\max}-1$ ) at the time index  $n$ . The first term and the second term in Eq. (8) are considered as accumulated path metric entering a state  $g_N$  and a branch metric from  $g'_N$  to  $g_{N+1}$ , respectively. Here, we define the path metric and branch metric as  $\varepsilon(g_N)$  and  $\zeta(g'_N \rightarrow g_{N+1})$ . An example of trellis diagram assuming  $G_{\max}=2$  is shown in Fig. 2.

The initial path metric for each state at sample index  $n=-1$  is set as  $\varepsilon(g_{-1})=0$ . At a particular time index  $n=N$  where  $0 \leq N \leq N_c-1$ , the branch metric is expressed by

$$\zeta(g'_N \rightarrow g_{N+1}) = \min_{c \in \Psi_{\text{mod}}^*} \left| \text{Re} \left\{ \left( \phi^*(g_{N+1}) \hat{d}(N+1) \right)^4 \right\} - \text{Re} \{c\} \right|. \quad (9)$$

Here, we change the phase rotation as a function of time index  $\phi(N+1)$  to  $\phi(g_{N+1})$ , which is the phase rotation value stored in the state  $g$  at time  $N+1$ . The path metric entering state  $g_{N+1}$  is selected by the following criterion.

$$\varepsilon(g_{N+1}) = \min_{g'_N=0 \sim G_{\text{max}}-1} (\varepsilon(g'_N) + \zeta(g'_N \rightarrow g_{N+1})). \quad (10)$$

Note that the selection of paths and branches in Eqs. (9) and (10) are repeated until  $n=N_c-1$ . Once the selection is done until  $n=N_c-1$ , the surviving path metric which corresponds to an optimal state number  $g_{n,\text{opt}}$  and optimal phase sequence  $\{\Phi_{\text{opt}}(n) = \phi(g_{n,\text{opt}}); n=0 \sim N_c-1\}$  can be determined by backward computation as follows.

$$g_{N_c-1,\text{opt}} = \arg \min_{g_{N_c-1}=0 \sim G_{\text{max}}} \varepsilon(g_{N_c-1}), \quad (11a)$$

$$g_{n',\text{opt}} = \arg \min_{g_n=0 \sim G_{\text{max}}} (\varepsilon(g_{n'}) + \zeta(g_{n'} \rightarrow g_{n'+1,\text{opt}})), \quad (11b)$$

where  $n' = N_c-2, N_c-3, \dots, 0$ . Since the blind SLM uses 2-value phase rotation,  $G_{\text{max}}$  can be set as  $2^P$  where  $P$  is the time memory of a state (i.e., a particular state  $g_n$  is determined as a set of phase rotation for time index  $n-P-1, n-P-2, \dots, n$ ). The algorithm in Eqs. (9)-(11) can be used without changes but it needs to start from index  $n=P-1$ .

Besides constructing the trellis diagram based on Eqs. (7)-(11), we utilize the phase rotation sequence codebook and remove the redundant branches and states prior to the estimation [7]. Fig. 3 shows an example of a trellis constructed by setting  $N_c=32$  and  $M=16$ , where we can observe that the trellis diagram is sparse and the use of 2-level phase set requires less number of branches and states than that of 3-level phase set, consequently requires lower complexity than the full trellis diagram. It was also discussed in [7] that an increasing of  $G_{\text{max}}$  can improve the estimation accuracy, but simultaneously increases the complexity due to many surviving branches and states.

**Table 1** Simulation parameters.

<b>Data transmission</b>	Data modulation	16QAM
	No. of subcarriers	$N_c=256$
	CP length	$N_g=16$
<b>SLM algorithm</b>	Phase rotation type	Random
	No. of phase sequences	$M=1 \sim 1024$
<b>User equipment</b>	Channel estimation	Ideal
	No. of UE antennas	$N_{\text{UE}}=1,2$
	Channel estimation	Ideal
<b>Base station</b>	No. of BS antennas	$N_{\text{BS}}=1,4$
	Receive filter	MMSE-FDE
<b>Channel</b>	Fading	Frequency-selective block Rayleigh
	Power delay profile	Symbol-spaced, 16-path uniform

**Table 2** Computational complexity per transmit block (16QAM).

	No. of real-valued multiplications	No. of real-valued additions
ML estimation, original [5]	$M \times (36N_c+1)$	$M \times (51N_c)$
ML estimation, fourth-order [9]	$M \times (15N_c+1)$	$M \times (12N_c)$
2-step estimation, original [7]	$38 \times N_{\text{total-branch}}$	$(51 \times N_{\text{total-branch}}) + MN_c$
2-step estimation, fourth-order	$17 \times N_{\text{total-branch}}$	$(12 \times N_{\text{total-branch}}) + MN_c$

**Remarks:**  $N_{\text{total-branch}}$  is the number of branches used in Viterbi algorithm per one transmit block (maximum is  $729 \times N_c$ )

### 3.2. Verification and correction

The Viterbi algorithm in Sect. 3.1 is aiming at selecting the path and the corresponding phase rotation sequence which provide the lowest distance from the fourth-order constellation. Therefore, there exists probability that the resultant sequence  $\{\Phi_{\text{opt}}(n); n=0 \sim N_c-1\}$  is not in the predefined codebook due to frequency-selective fading and noise [7]. Here, verification and correction are introduced for checking the similarity between  $\{\Phi_{\text{opt}}(n)\}$  and the existing sequences in the codebook. We can use the Hamming distance as the indicator since the difference in rotation angle does not affect the data detection error.

Let  $\{\Phi_{\text{opt}}(n); n=0 \sim N_c-1\}$  denote the resultant phase rotation sequence obtained from the Viterbi algorithm. The estimated phase rotation sequence to be used in de-mapping  $\{\Phi_{\tilde{m}}(n); n=0 \sim N_c-1\}$ , with the corresponding sequence index  $\tilde{m}$ , can be determined by

$$\begin{aligned} \tilde{m} &= \arg \min_{m=0 \sim M-1} \left( b(\{\Phi_{\text{opt}}(n)\}, \{\Phi_m(n)\}) \right) \\ &= \arg \min_{m=0 \sim M-1} \left( \{\Phi_{\text{opt}}(n)\} \oplus \{\Phi_m(n)\} \right), \end{aligned} \quad (12)$$

where  $b(\{A\}, \{B\})$  denotes the Hamming distance between sequence  $A$  and  $B$  and  $\oplus$  is exclusive or operation [11]. Finally, the soft-decision data symbol after de-mapping and before de-modulation  $\{\tilde{d}(n); n=0 \sim N_c-1\}$  is obtained by  $\{\tilde{d}(n) = \Phi_{\tilde{m}}^*(n) \hat{d}(n); n=0 \sim N_c-1\}$ . Note that when the STBC-TD is used, the estimated phase rotation sequence should be indexed with  $j$  as  $\{\Phi_{\tilde{m}(j)}(n); n=0 \sim N_c-1\}$ , with the corresponding sequence number  $\tilde{m}(j)$ ,  $j=0 \sim J-1$ .

### 4. Performance evaluation

Simulation parameters are summarized in Table 1. Single-user SC uplink using SISO or STBC-TD are assumed in this paper, while channel coding is not considered for simplicity. Path loss and shadowing loss are not considered. Note that the performance evaluation of blind SLM in MU-MIMO transmission is left as future works. Phase rotation codebook are generated randomly as  $\Phi_m(n) \in \{e^{j0}, e^{j(2\pi/3)}, e^{j(4\pi/3)}\}$  for conventional blind SLM using 3-level phase rotation set and the estimation based on original QAM mapping, and  $\Phi_m(n) \in \{e^{j0}, e^{j(3\pi/4)}\}$  for the modified blind SLM. Performance evaluation is discussed in terms of PAPR, BER and computational complexity, and

then compared with the conventional blind SLM in [4-7] using either ML or 2-step phase rotation sequence estimation, but based on original QAM constellation.

#### 4.1. PAPR vs computational complexity

PAPR performance is evaluated by measuring the PAPR value at complementary cumulative distribution function (CCDF) equals  $10^{-3}$ , called  $\text{PAPR}_{0.1\%}$ . Computational complexity is evaluated by counting the number of real-valued addition operations and assuming that the complexity of real-valued multiplication is approximately 3 times of real-valued addition [12]. The total complexity of phase rotation sequence estimation is summarized in Table 2. The complexity of 2-step estimation based on original constellation is calculated using Viterbi algorithm with  $G_{\max}=27$  [7]. In addition, the complexity of modified blind SLM is evaluated by setting  $G_{\max}=8$ .

Fig. 4 shows the  $\text{PAPR}_{0.1\%}$  versus total computational complexity of SC uplink STBC-TD using blind SLM. Transmission scheme with the tradeoff mark in the bottom-left of Fig. 4 means it can achieve low PAPR with low-complexity phase rotation sequence estimation. PAPR reduces when  $M$  increases in all schemes, but the total complexity also increases. The use of 2-step estimation with original constellation can reduce the complexity while maintaining the same PAPR as that of conventional blind SLM with ML estimation in [5], but the complexity reduction capability becomes obvious only when  $M>64$ . The use of ML estimation with fourth-order constellation [9] can reduce the complexity even when  $M\leq 64$  due to less number of signal points in the minimum Euclidean distance calculation. However, the complexity of ML estimation using fourth-order constellation becomes higher than 2-step estimation using original constellation when  $M>64$ . This is because the complexity of ML estimation is a function of  $M$ , while the complexity of 2-step estimation mostly depends on  $N_{\text{total-branch}}$ , which is almost constant when  $M$  is large.

The modified blind SLM achieves the same PAPR as that of conventional blind SLM but requires much less computational complexity at the receiver. The use of 2-level phase set can set  $G_{\max}$  to be less than that of 3-level phase set at the same number of time memory (i.e.  $3^3=27$  for 3-level phase set but only  $2^3=8$  for 2-level phase set). Moreover, the use of fourth-order constellation reduces the number of signal points considered in branch metric calculation and consequently contributes to complexity reduction [8,9]. Assuming  $N_c=256$ ,  $M=256$  and  $G_{\max}=8$ , the modified blind SLM can lower the PAPR by 3.0 dB compared to the conventional SC uplink STBC-TD. The required computational complexity of phase rotation estimation in the modified blind SLM is only 3% of the ML estimation using original constellation [5], 9% of the ML estimation using fourth-order constellation [9], and 10% of the 2-step estimation using Viterbi algorithm based on the original QAM constellation [7].

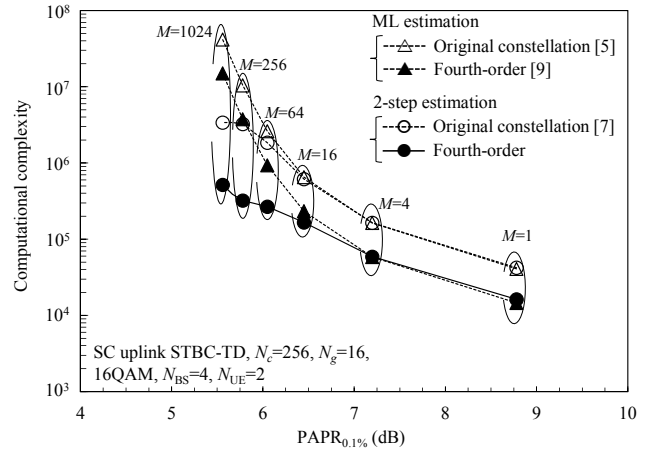


Fig. 4  $\text{PAPR}_{0.1\%}$ -complexity tradeoff.

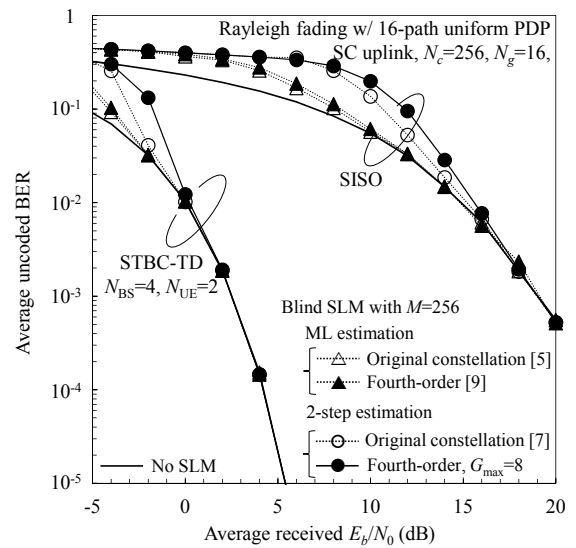


Fig. 5 BER performance.

In addition, it is interesting to observe that the complexity of modified blind SLM remains similar when  $64 < M \leq 256$  since  $N_{\text{total-branch}}$  is almost constant. However, the complexity increases when  $M=1024$ . This is because the large size of codebook requires high computational complexity in the second step (verification and correction), indicating that the complexity when  $M$  is relatively large relies on the second step than the first step.

#### 4.2. BER performance

Fig. 5 shows the average uncoded BER performance of SC uplink SISO and STBC-TD with  $N_{\text{BS}}=4$  and  $N_{\text{UE}}=2$  and equipped with blind SLM as a function of average received bit energy-per-noise power spectrum density ( $E_b/N_0$ ). The BER performances of transmission without blind SLM and the conventional blind SLM in [5], [7] and [9] are also plotted for comparison. The number of available phase rotation sequences is set to be  $M=256$ .

Firstly, it is seen that the use of blind SLM with phase rotation sequence estimation achieves worse BER than that of without blind SLM in every scheme when the  $E_b/N_0$  is low (i.e.,  $E_b/N_0 < 16$  dB for SISO and  $E_b/N_0 < 0$  dB for

STBC-TD). This is because the impact from fading and noise leads to the difficulty in classification between the symbols obtained from correct de-mapping and that of incorrect de-mapping. However, there is no significant BER degradation when either the ML estimation based on original constellation [5], ML estimation based on the fourth-order constellation [9], 2-step estimation based on original constellation [7], or the modified blind SLM is used. This emphasizes the attractiveness of the modified blind SLM since it achieves low-complexity estimation without significant degradation on BER and PAPR.

It is also observed from Fig. 5 that the 2-step estimation based on fourth-order constellation achieves the worst BER at low- $E_b/N_0$  region. This can be described by referring the fourth-order constellation of 16QAM symbols obtained from correct and incorrect de-mapping in [9]. Although 1 out of 4 mapping points can produce large Euclidean distance (i.e., error magnitude) when the de-mapping is incorrect, the rest of mapping points produce relatively small error magnitude. The above fact leads to false branch selection in Viterbi algorithm.

## 5. Conclusion

In this paper, we aim at achieving a low-complexity phase rotation sequence estimation even when  $M$  is large. We introduced a modified blind SLM using the 2-level phase rotation set  $\{0^\circ, 135^\circ\}$  and the 2-step sequence estimation based on the fourth-order constellation. Our modified blind SLM with the 2-level phase rotation set and the 2-step sequence estimation using Viterbi algorithm and the fourth-order constellation achieves low computational complexity due to the following reasons; reduction of branches and states in Viterbi algorithm (contributed by the use of 2-level phase set) and reduction of possible paths to be considered during survival path searching (contributed by the use of fourth-order constellation). Simulation results confirmed that our modified blind SLM can reduce the PAPR of SC uplink by 3.0 dB when  $M=64$ . The computational complexity of phase rotation sequence estimation when  $N_c=256$ ,  $M=256$  and  $G_{\max}=8$  is only 3% of the ML estimation using original constellation [5], 9% of the ML estimation using fourth-order constellation [9], and 10% of the 2-step estimation using original constellation [7]. It was also confirmed that there is no significant BER degradation compared to the transmission without blind SLM when the received  $E_b/N_0 > 16$  dB for SISO transmission and  $E_b/N_0 > 0$  dB for STBC-TD transmission, respectively.

In addition, our modified blind SLM can be applied to OFDM downlink and also MU-MIMO transmission (both SC uplink and OFDM downlink) without major modification.

## Acknowledgement

This paper includes a part of results of “The research and development project for realization of the fifth-generation mobile communications system” commissioned to Tohoku

University by The Ministry of Internal Affairs and Communications (MIC), Japan.

## References

- [1] 5GMF White Paper, *5G Mobile Communications Systems for 2020 and beyond*, Ver. 1.01, Jul. 2016.
- [2] H. G. Myung, J. Lim and D. J. Goodman, “Single Carrier FDMA for Uplink Wireless Transmission,” *IEEE Veh. Technol. Mag.*, Vol. 1, No. 3, pp. 30-38, Sept. 2006.
- [3] S. Kumagai, T. Obara, T. Yamamoto and F. Adachi, “Joint Tx/Rx MMSE Filtering for Single-Carrier MIMO Transmission,” *IEICE Trans. Commun.*, Vol. E97-B, No. 9, pp. 1967-1976, Sept. 2014.
- [4] A. Boonkajay and F. Adachi, “A Blind Polyphase Time-Domain Selected Mapping for Filtered Single-Carrier Signal Transmission,” *Proc. IEEE Veh. Technol. Conf. (VTC2016-Fall)*, Montréal, Canada, Sept. 2016.
- [5] A. Boonkajay and F. Adachi, “PAPR Reduction for STBC Transmit Diversity with Transmit FDE using Blind Selected Mapping,” *Proc. IEEE VTS Asia Pacific Wireless Commun. Symp. (APWCS2017)*, Incheon, Korea, Aug. 2017.
- [6] A. Boonkajay and F. Adachi, “A Stream-wise Blind Selected Mapping Technique for Low-PAPR Single-Carrier Uplink MU-MIMO,” *Proc. IEEE/CIC Int. Conf. on Commun. in China (IEEE/CIC ICC2017)*, Qingdao, China, Oct. 2017.
- [7] A. Boonkajay and F. Adachi, “2-Step Phase Rotation Estimation for Low-PAPR Signal Transmission using Blind Selected Mapping,” *Proc. IEEE Int. Symp. On Personal, Indoor and Mobile Radio Commun. (PIMRC2017)*, Montreal, Canada, Oct. 2017.
- [8] C. Siegl and R. Fischer, “Selected Mapping with Implicit Transmission of Side Information using Discrete Phase Rotations,” *Proc. Int. ITG Conf. on Source and Channel Coding (SCC2010)*, Siegen, Germany, Jan. 2010.
- [9] A. Boonkajay and F. Adachi, “A Low-Complexity Phase Rotation Estimation using Fourth-Power Constellation for Blind SLM,” *To be presented at IEEE Veh. Technol. Conf. (VTC2018-Fall)*, Chicago, USA, Aug. 2018.
- [10] A. Viterbi, “Error Bound for Convolutional Codes and an Asymptotical Optimum Decoding Algorithm,” *IEEE Trans. Inform. Theory*, Vol. 13, No. 2, pp. 260-269, Apr. 1967.
- [11] Henry S. Warren, *Hacker’s Delight*, 2<sup>nd</sup>-ed., Addison Wesley, 2012.
- [12] S. Arora and B. Barak, *Computational Complexity: A Modern Approach*, Cambridge, 2009.